archaeometry

Archaeometry **54**, 4 (2012) 623–642 doi: 10.1111/j.1475-4754.2011.00648.x

NON-DESTRUCTIVE SOURCING OF BRONZE AGE NEAR EASTERN OBSIDIAN ARTEFACTS: REDEVELOPING AND REASSESSING ELECTRON MICROPROBE ANALYSIS FOR OBSIDIAN SOURCING*

E. FRAHM

Department of Earth Sciences, University of Minnesota, 310 Pillsbury Drive SE, Minneapolis, Minnesota 55455, USA

Despite predictions in the 1980s that electron microprobe analysis (EMPA) would become a popular technique for obsidian sourcing, few studies have used it with this goal, and most of them are now outdated and unrepresentative of modern EMPA. For example, Merrick and Brown (1984) recorded their data on punch cards. Furthermore, these studies destructively prepared artefacts for analysis. The research at hand endeavoured: (1) to establish the modern capabilities of EMPA for obsidian sourcing; and (2) to develop and evaluate procedures for non-destructive artefact analysis. Issues such as diagenetic effects and compatibility with NAA and XRF data were also investigated.

KEYWORDS: OBSIDIAN, NON-DESTRUCTIVE, SOURCING, ELECTRON MICROPROBE ANALYSIS, BRONZE AGE, SYRIA

INTRODUCTION

The earliest successes in obsidian sourcing used optical emission spectroscopy (OES) (e.g., Cann and Renfrew 1964), which was, at best, semi-quantitative and necessitated 'grinding up the samples with pestles and mortars' (Renfrew, in Bradley 1993, 74). OES was soon replaced by neutron activation analysis (NAA) (Gordus *et al*. 1967) and X-ray fluorescence (XRF) (Stevenson *et al*. 1971), which have dominated obsidian sourcing ever since and proven highly effective. The Archaeometry Laboratory of the University of Missouri Research Reactor (MURR) has continued to refine NAA for obsidian sourcing, while the Geoarchaeological XRF Laboratory at Berkeley, the Northwest Research Obsidian Studies Laboratory, and the Geochemical Research Laboratory have done the same for XRF. Collectively, researchers at these four laboratories have sourced over 100 000 artefacts, attesting to the efficacy of these techniques.

Nevertheless, NAA and XRF do have limitations. Destructive specimen preparation and handling is a major limitation of NAA. Artefacts are irradiated intact or sampled by drilling or cutting. The intact artefacts, though, must be discarded as radioactive waste or stored until their radioactivity reaches safe levels. Ideally, specimens for XRF are ground into powders, but entire artefacts can be analysed. XRF, though, has a well-known specimen-size limit. Artefacts smaller than a few millimetres in diameter or thickness yield errors, imposing a size bias. NAA also has size limits. Specimen sizes of 100 mg (roughly 40 mm^3) or greater are common; however, using special procedures, specimens as small as 5 mg (2 mm^3) may be analysed (Eerkens *et al*. 2002).

The depth and breadth of NAA- and XRF-generated obsidian databases are unmatched, so ideally new analytical techniques brought to obsidian sourcing should not only (1) demonstrate compatibility with NAA and XRF data, but also (2) address the limitations of NAA and/or XRF.

*Received 10 June 2011; accepted 14 July 2011

The last decade of obsidian sourcing has seen an increase in the use of spot analytical techniques, in which a laser or particle beam is focused on to an artefact to create a spectrometric signal. These primarily include particle-induced X-ray/gamma-ray emission (PIXE–PIGME; e.g., Summerhayes *et al*. 1998), secondary ion mass spectrometry (SIMS; e.g., Anovitz *et al*. 1999), and laser-ablation inductively coupled plasma mass spectrometry (LA–ICP–MS; e.g., Carter *et al*. 2006). LA–ICP–MS, in particular, has gained popularity because it offers micro-destructive analyses (i.e., the laser leaves pits typically tens to hundreds of microns across and deep), induces no radioactivity and enables sourcing of artefacts too small for NAA or XRF.

Electron microprobe analysis (EMPA) is another spot technique that, despite early predictions that it would become popular (Freestone 1982; Kempe and Templeman 1983), has largely remained on the periphery of obsidian sourcing. Instead of an ablating laser, an electron beam is focused on to a specimen to generate characteristic X-rays. These electrons induce no radio-activity and leave no pits. With a spot size as small as 1–2 μm, EMPA is prevalent in tephrochronology for analysing glass shards in volcanic ash. Under favourable conditions, specimens can be analysed without cutting, grinding or polishing. Prior studies using EMPA for obsidian sourcing, though, have not established that artefacts can be analysed non-destructively. Furthermore, these earlier studies are not indicative of the state of the art. Therefore, my goals here are to report: (1) the accuracy, repeatability and validity of modern EMPA for obsidian sourcing, given appropriate choices; and (2) the development and evaluation of analytical procedures for non-destructively sourcing artefacts from, in this case, Tell Mozan. An overview of EMPA is beyond the scope here, so readers are encouraged to consult Reed (1993, 2005) and Goldstein *et al*. (2003).

Tell Mozan is the site of a Bronze Age Hurrian urban centre in northeastern Syria. The lithic assemblage is dominated by prismatic blades and bladelets. The longest obsidian blades are over 80 mm, and the smallest bladelets are only 10 mm long and 1 mm thick. There are also geometric microliths, scrapers, points and borers. Debitage, including millimetre-scale debris, has been recovered as well. Obsidian artefacts small enough for export are below the XRF size limit, and because the permit stipulated non-destructive study and timely return of the artefacts, NAA was not an option either. Here, I demonstrate how EMPA is a viable alternative for non-destructively sourcing artefacts from long blades to tiny debris. EMPA offers an accuracy and repeatability that rivals other techniques for many elements. Furthermore, as a major technique in the geosciences, it is available at many universities for competitive rates. This research was conducted using the JEOL 8900 SuperProbe at the Electron Microprobe Laboratory, Department of Earth Sciences, University of Minnesota–Twin Cities.

Non-destructive EMPA for obsidian sourcing faces four main challenges, and this paper examines my procedures to mitigate these challenges. These procedures are considered in light of earlier research, evaluated using a framework first suggested by Hughes (1998) and re-derived elsewhere (Frahm, 2010, in press), and applied to a series of artefacts from Tell Mozan. It is outside the scope of this paper to consider the entirety of the results and their interpretation, but the source assignment for one artefact is presented here in detail to demonstrate that non-destructive EMPA is, indeed, valid for obsidian sourcing.

THE ROLE OF CHOICE

The role of choice in EMPA has long been recognized (e.g., Goldstein *et al*. 1981, v). Long (1995) explains ‘the stability of the primary beam and of the spectrometer and detector are clearly important . . . but [so is] the expertise of the operator in choosing and setting the optimum operating conditions’ (15). Lifshin and Gauvin (2001) even offer a ‘process map’ (basically an

operational sequence or *chaîne opératoire*) of steps at which a researcher makes choices. One starts with an initial analytical scheme in mind, feedback from observations changes the scheme, a modified scheme yields new feedback and so on. These actions form a sequence informed by a researcher's theoretical and practical 'know-how'. Consequently, I highlight the choices made to develop EMPA specifically for non-destructive obsidian sourcing, and I contrast them with choices made in previous EMPA-based studies.

Earlier EMPA-based sourcing studies

Few studies have used EMPA for obsidian sourcing, most notably Merrick and Brown (1984) in East Africa, Weisler and Clague (1998) in Hawaii, and Tykot (1995, *inter alia*) in the Mediterranean and elsewhere (e.g., Tykot and Chia 1997; Rosen *et al*. 2005). Two studies reportedly used a 'microprobe', but actually they utilized scanning electron microscopy with energy-dispersive spectrometry (SEM–EDS) (Biró and Pozsgai 1984; Keller and Seifried 1990). Two other collaborations have presented work on EMPA-based obsidian sourcing in Japan (e.g., Wada 2009) and the Western Mediterranean (Le Bourdonnec *et al*. 2005, 2010; Sanna *et al*. 2010). Their conference papers were too recent to affect the research here, and hopefully future publications will provide more details regarding their approaches, procedures and evaluation.

The related technique of SEM–EDS is also occasionally used for obsidian sourcing, often supplemented by other techniques (Abbès *et al*. 2003), or in studies that did not analyse even one artefact (Acquafredda *et al*. 1996, 1999; Le Bourdonnec *et al*. 2006). Consequently, it is difficult to assess its modern application to obsidian sourcing. In one recent study of obsidian artefacts at Çatalhöyük (Poupeau *et al*. 2010), though, SEM–EDS did not distinguish the East Göllü Dağ and West Acıgöl sources. In general, EMPA has better repeatability, sensitivity and X-ray resolution than SEM–EDS, which is somewhat faster and more widely available. Thus my findings are not necessarily representative of SEM–EDS, particularly when used non-destructively, and I discuss SEM–EDS here only with respect to artefact preparation (or the lack thereof).

Earlier studies that used EMPA do not represent its modern capabilities. The best-known study, Merrick and Brown (1984), used an ARL-EMX, a microprobe from the 1960s. The data were output on punch cards, and the researchers selected the simplest data-correction algorithm to avoid excessive mainframe user fees. Today, more sophisticated algorithms correct raw data instantaneously, and one has immediate feedback from a specimen, allowing further refinement of the procedures. Thus Merrick and Brown (1984) is no more representative of modern EMPA than Gordus *et al*. (1967) of NAA or Stevenson *et al*. (1971) of XRF today.

These prior studies also involve different priorities and, hence, procedures. Merrick and Brown (1984) put a priority on speed, so they measured three elements with high concentrations (≥0.1 wt%) and analysed 260 artefacts in 6 h (1.4 min per artefact). Tykot (1995), though, sought more elements (9–11) at lower concentrations (≥0.01 wt%), so he analysed artefacts and geological specimens for about 6 min each.

My priorities included establishing the maximum accuracy, repeatability and sensitivity of EMPA for obsidian. Because Merrick and Brown (1984) had already shown that EMPA can be quick, time was given a lower priority. Consequently, over 900 geological specimens and 100 artefacts were each analysed for 20 elements over nearly 2 h (i.e., 20 5-min analyses for each). Three points should be made with respect to the analytical time. First, although XRF can measure element concentrations in minutes, the artefacts of interest were too small for XRF. Second, EMPA is often available for academic researchers at low off-peak rates (e.g., $10 per hour at the

University of Minnesota), so the cost per artefact is competitive. Third, having established the limits, subsequent analytical times have been cut in half.

I present the analytical choices made in these earlier studies—from specimen preparation to data processing—to emphasize recent advances in EMPA and the role of choice in analytical procedures while building on their important foundational work. When relevant, I will also refer to analytical choices made in EMPA-based tephrochronology.

Specimen preparation

Artefacts were only prepared destructively in earlier EMPA-based studies. Merrick and Brown (1984) mounted 'fragments of obsidian artefacts' in epoxy, requiring 'minor damage' to artefacts (230, 231). Tykot (1995) removed a '1–2 mm sample . . . by flaking or using a high-speed diamond saw' and mounted it in epoxy (111, 126). Weisler and Clague (1998) prepared artefacts as thin sections (116). Studies using SEM–EDS either prepared the artefacts destructively (Biró and Pozsgai 1984), reportedly attempted non-destructive analysis but offered no results (Biró *et al*. 1986; Abbès *et al*. 2003), studied only geological specimens (Acquafredda *et al*. 1996, 1999; Le Bourdonnec *et al*. 2006) or reported only partial success (Poupeau *et al*. 2010).

In this study, the artefacts were not ground, polished, cut, chipped or otherwise altered in morphology. Preparation of any sort was minimal. Artefacts were lightly cleaned with isopropyl alcohol (IPA) and KimWipes tissues to remove fingerprints. A thin carbon layer, about 15 nm thick, gave each artefact an electrically conductive coat, and it was later removed using IPA. Carbon coating is a standard procedure for EMPA of geological specimens (Reed 1993, 156; Goldstein *et al*. 2003, 669; Reed 2005, 156), and it is well established that the carbon has minuscule effects on the X-ray and electron signals (Kerrick *et al*. 1973).

Elements

Each element to be quantified must be chosen beforehand. I conducted two rounds of analysis on each artefact and geological specimen. The first round consisted of 14 elements abundant in igneous rocks: Si, Ti, Al, Cr, Fe, Mn, Mg, Ca, Na, K, P, F, S and Cl. These were considered the 'geologically major elements', even though some of their concentrations are below 0.1% in obsidian. Tests of additional elements identified six candidates for the second round: Zr, Nb, Ga, Zn, Ba and Ce. These were considered the 'trace elements', although the concentrations of Zr and Ba sometimes are above 0.1%.

Accelerating voltage

An accelerating voltage (i.e., the voltage applied to the electron beam) must be chosen by a researcher. Too low a voltage leaves the electrons with insufficient energy to generate X-rays, and too high a voltage yields undesirable effects, such as additional heat and greater reliance on the data correction algorithms. A voltage of 15 kV is commonly chosen to balance these effects in geological specimens. The three prior EMPA-based obsidian sourcing studies all used 15-kV accelerating voltages. This is also the norm in tephrochronology (e.g., Allan *et al*. 2008; Payne *et al*. 2008), with higher (20 kV in Hang *et al*. 2006) or lower (13 kV in Tryon *et al*. 2009) voltages being rare. Therefore, I used 15 kV in the present research.

Beam current

The beam current (i.e., the number of electrons in the beam) must also be chosen. For routine geological research, currents of 20–30 nA are most common. A high current produces high X-ray

intensities, but there are two main limitations. First, Na and K are susceptible to migration under an intense beam, especially in obsidian. This can be mitigated using a broad beam. Second, under high beam currents, excessive X-ray intensities for major elements may yield inaccurate results due to an over-reliance on imperfect corrections to the raw counts (i.e., error in the spectrometer dead-time corrections is amplified; Reed 2005, 112). Tests revealed that this occurred above 80 nA for Si in obsidian.

Beam currents in prior studies vary. Merrick and Brown (1984) chose 50 nA, whereas Weisler and Clague (1998) used 10 nA. Tykot (1995) does not report his current choice. In tephrochronology, beam currents vary from 4 nA (Adams *et al*. 2006) to 100 nA (Smith *et al*. 1977). After initial experiments, I chose 50 nA for the major-element round and 600 nA for the trace-element round. Such high currents were possible only because I (a) separated the major- and trace-element analyses into two rounds and (b) defocused the beam.

Beam diameter

One can defocus the beam and analyse a larger spot for migration-prone specimens; however, too broad a beam increases the error due to precise geometric requirements (Reed 2005, 144). Various beam diameters are used in tephrochronology, usually limited by the shard sizes. Payne *et al*. (2008) used a 1-μm beam (and consequently produced data with totals below 95%). Most researchers use a 5-μm (e.g., Tryon *et al*. 2009) or a 10-μm beam (e.g., Adams *et al*. 2006). Broader beams, such as 20 μm (e.g., Allan *et al*. 2008) or 30 μm (e.g., Hanson *et al*. 1996), are uncommon.

Based on tests of Lipari obsidian using various beam currents and diameters, Hunt and Hill (2001) concluded that the Na and K values were accurate when the surface power density was 2.3 W mm^{-2} or less at the analysis spot. Thus this was a target for my major-element round. In comparison, Merrick and Brown (1984) had a nearly identical power density (2.4 W mm^{-2}), but Weisler and Clague (1998) had a density three times greater (7.5 W mm^{-2}), suggesting that their Na and K data were affected. After initial tests, I chose a 30-μm beam, meaning that the power density for the major-element round was only 1.1 W mm^{-2}.

Counting times

The time taken to count the characteristic and background X-rays must also be selected. For routine EMPA, 10 s on the characteristic X-ray 'peak' and 5 s on each of two background measurements is often sufficient for a repeatability of ±1% relative (Reed 2005, 77). Merrick and Brown (1984) used count times of 10–12 s, but it is unclear how the time was divided between peak and background measurements (if at all). Tykot (1995) counted for 10–80 s per element, but there is also no elaboration. The counting times of Weisler and Clague (1998) are unreported. Tephrachronologists report counting times ranging from 10 s (e.g., Hang *et al*. 2006) to 40 s (e.g., Tryon *et al*. 2009) per element.

To maximize repeatability, for the major elements, I used 25 s on the X-ray peak and 25 s on each background measurement (75 s in total). Only Na was counted for only 10 s on the peak and 10 s on each background so that any migration effects were minimized. For the trace-element round, I utilized 50 s on the peak and 50 s on each background measurement (150 s in total).

Number of analyses

When using a spot analytical technique such as EMPA or LA–ICP–MS, mineral inclusions within the obsidian must be avoided, or their compositions will contribute to the analysis (i.e., if a

magnetite grain lies within the spot, the measured Fe will be too high and all other elements too low). Consequently, most researchers using spot techniques acquire multiple analyses, typically three, on each specimen. For example, Tykot (1995) analysed 'three points per sample . . . in case a phenocryst contributed' (113).

I analysed at least 20 spots on each specimen and artefact between the major- and trace-element rounds ($\mu = 27$), and any mineral inclusions were avoided using electron and reflected-light microscopy. The goal was to maximize repeatability, not account for any heterogeneities. X-ray emission is a random, statistical process and sequential measurements exhibit a Gaussian distribution. Therefore, the central limit theorem applies with sufficient analyses, and the means were considered the most probable values. Sensitivity improved as well. Detection limits of 20 ppm have been reported with 30-min counting times (Goldstein *et al*. 2003, 447); however, on such timescales, heat-induced damage becomes an issue. In terms of counting statistics, 10 2.5-min analyses are equivalent to one 25-min analysis, but the obsidian needs to be stable for less than 3 min under the beam.

Calibration standards

Quantitative EMPA is a comparative method. X-rays are measured from the specimen and standards under the same conditions. Corrections for various physical effects are applied to the raw counts, resulting in an assay of the elements' concentrations in the specimen. Choosing standards is complex (Reed 1993, 159; Reed 2005, 128) and the choices often go unreported. Merrick and Brown (1984) apparently used obsidians as standards. Weisler and Clague (1998) reported only 'natural and synthetic standards' and Tykot (1995) simply cited 'international standards'. Tephrachronologists often make similarly vague statements (e.g., 'calibrated using a sequence of minerals and metals'; Payne *et al*. 2008).

The importance of similar compositions between the standards and specimens is roughly proportional to an element's concentration. As concentrations decrease, good counting statistics become more important than similar compositions. For example, Cl is present in Smithsonian obsidian standard VG-568, but at 0.1 wt%, this is too low a concentration for standardization. Thus natural glasses were used for major elements, silicates for minor elements, and synthetic glasses and compounds for trace elements when necessary. My major-element standards were rhyolite (Smithsonian VG-568), basalt (USNM 113498 and 113716) and tektite (USNM 2213) glasses for Si and Al; hornblende (USNM 143965) for Mg, Ca, Ti and Fe; albite (Harvard 131705) for Na; microcline (UC 258) for K; chromite (USNM 117075) for Cr; hortonolite (UC 27) for Mn; apatite (USNM 104021) for F and P; meionite (USNM R6600-1) for Cl; and pyrite for S. My trace-element standards were gahnite (USNM 145883) for Zn; GaAs for Ga; zircon (USNM 117288-3) for Zr; Nb metal for Nb; Corning C glass for Ba; and REE3 glass for Ce. Matrix corrections (JEOL's ZAF scheme) were applied to every standard, geological specimen and artefact to account for differences in atomic number, X-ray absorption and secondary X-ray fluorescence.

Data correction and reporting

As noted above, raw X-ray counts must be corrected for various physical effects to be converted into element concentrations. Merrick and Brown (1984) used simple linear regression to save on computing fees, but their concerns are now obsolete. Tykot (1995) and Weisler and Clague (1998) utilized the Bence–Albee scheme, a set of empirical coefficients devised before computers were

fast enough to calculate the corrections. JEOL's ZAF correction scheme is a modern correction model derived from first principles and large databases.

Some using EMPA chose to normalize their data to 99% or 100% (Tykot 1995; Tykot and Chia 1997), ostensibly to account for variable water content. Normalization is generally considered unacceptable in EMPA as it can obscure, or even increase, error (Goldstein *et al*. 2003, 421; Reed 2005, 125). Consequently, I report the data with each element independently calibrated to standards. These data are unprocessed beyond (1) applying the ZAF correction algorithms and (2) averaging the multiple analyses for each specimen.

Miscellaneous procedures

Additional procedures improved the accuracy and repeatability. First, to select suitable background measurement locations, I conducted full X-ray spectrum scans on obsidian to search for interferences. Second, spectrometers may 'drift' slightly over time, so they were 'repeaked' for abundant elements every 5–10 analyses. Third, an autofocus system assured that artefacts were precisely positioned in the focal plane during measurement. Fourth, Na and K were measured first to minimize any migration effects. Two modifications to the proprietary software also increased the trace-element repeatability: it was changed to report (1) concentrations to four decimal places to better calculate means and (2) negative concentration data. This latter is important because, for trace elements, one 'tail' of the Gaussian distribution can fall into the negative range, and including the negative values allows the correct mean to be calculated.

Challenges to non-destructive artefact analyses

There were four main challenges to overcome for conducting non-destructive EMPA of obsidian artefacts. The first two challenges involve specimen requirements, while the third and fourth involve post-depositional effects on artefacts' surfaces.

Challenge 1: non-flat artefact surfaces The first challenge was that obsidian artefacts do not have flat surfaces. EMPA data correction algorithms assume that the beam is perfectly perpendicular to the specimen surface, but conchoidal fracturing produces only curved surfaces. Fortunately, the radii of the flake scars are several millimetres or centimetres, so on a micrometre scale (three or four orders of magnitude smaller), certain areas within the scars are effectively flat and perpendicular to the beam. The visible-light microscope, common on modern microprobes, is outfitted with a crosshair reticule as a means of identifying its optic axis and focal plane, which coincide with those of the electron beam. Consequently, this microscope can (1) reveal if a small area on a specimen was tilted more than 2–3° (determined experimentally using geometry and the optically encoded stage) and (2) permit exact positioning of the artefact surfaces in the optimal plane for analysis.

Challenge 2: non-polished artefact surfaces Specimens for EMPA ideally have mirror-like surfaces; however, the artefacts remained unpolished. Fortunately, obsidian fracture surfaces are extremely smooth. Under a reflected-light microscope, chert surfaces appear rough and dark, but obsidian looks smooth and bright, interrupted only by small irregularities due to microscopic minerals (e.g., Hurcombe 1992, 24; Patel *et al*. 1998, 1052). Therefore, I was able to select smooth areas on the artefacts to analyse and avoid any mineral inclusions by watching for their surface aberrations.

Challenge 3: surface hydration Hydration is one of two surface effects that complicate non-destructive artefact analyses. Under the discussed conditions, characteristic X-rays were emitted from the topmost 2.0–2.5 μm of the surface. If the hydration rind is less than 1 μm deep, most X-rays would be emitted from the non-hydrated interior. If, though, the rind is deeper than 3 μm, the X-rays would be emitted entirely from the hydrated obsidian. The rind depths of the Tell Mozan artefacts were unknown at the outset. Estimates based on other studies varied from almost non-existent (Friedman *et al*. 1969) to several microns (Rosen *et al*. 2005). Two factors, though, worked in favour of the Tell Mozan artefacts having shallow rinds: they (1) date to the Bronze Age; and (2) they were buried in, at least what is currently, a semi-arid environment.

The effects of analysing hydrated obsidian were also uncertain at the outset. In a sense, the hydrated rind is simply 'diluted' with water. Water absorption disrupts the network of silica tetrahedra in obsidian, breaking Si–O–Si bonds and forming Si–O–H H–O–Si (Yanagisawa *et al*. 1997). The degree of dilution depends on the water content within the hydrated rind, reports of which vary from 2% (Friedman *et al*. 1969) to 10% (Anovitz *et al*. 1999).

If the hydration rind was less than 1 μm deep and contained 2% water, minimal effect would be expected. On the other hand, a 5-μm-deep rind with 10% water would be anticipated to have a pronounced effect, leading to analytical totals below 90%. Ultimately, totals of 97.0 ± 1.4% for the Tell Mozan artefacts suggest that the situation was closer to the former. This error source was mitigated by excluding the elements most likely to be affected by disruption of the glass network (e.g., Si, Na and K) from the subsequent data analysis.

Challenge 4: weathering Hydration is accompanied by diagenetic surface alteration, generally called weathering. Alkalis (e.g., Na, K and Rb), in particular, are mobile near the weathered surface (Coote and Nistor 1982). Recent studies have concluded that weathering is much shallower than the hydrated rind. Using SIMS on Mexican obsidian artefacts, Anovitz *et al*. (1999) concluded that 'the depths at which alkali concentrations become constant are significantly less than that of water' (742). In one Chalco artefact, for example, the hydration rind was 3.1 μm deep; however, Na, K and Ca reached their unaltered concentrations at about 0.3 μm. Similarly, Patel *et al*. (1998) analysed Sardinian obsidian using SIMS. They found Na and K were depleted at 0.1 μm, enriched at 0.2 μm and returned to their initial concentrations at about 0.4 μm, whereas Si and Al exhibited 'a near constant distribution' (1049). Furthermore, the depth plots in both studies hinted that, with depleted and enriched layers in the topmost 0.2–0.3 μm, there might actually be little net change in composition, especially when measured to a depth of 2.0–2.5 μm.

Therefore, weathering was anticipated to be an order of magnitude shallower than the hydration rinds, meaning that any effects on the data would be moderate. Moreover, it was known that all elements would not be affected equally. Relatively immobile elements were expected to remain largely unaffected and useful for sourcing. The elements most affected by weathering were identified by observing offsets between artefacts and geological specimens in scatterplots and, consequently, were excluded from the subsequent data analysis.

Evaluation framework

Hughes (1998) proposed a fourfold framework—precision, accuracy, reliability and validity—to assess obsidian sourcing procedures. This framework—re-derived and updated to include repeatability, accuracy, reproducibility and validity—is discussed in detail elsewhere (Frahm 2010, in press) and used here to evaluate my procedures.

Repeatability

Repeatability—that is, the degree to which measurements yield identical results with the same conditions, observer and instrument during a specific time (e.g., the analytical session, or the course of a particular study)—is determined by taking repeated analyses on a reference standard and quantified by the relative standard deviation. For EMPA, repeatability depends on counting statistics, instrument stability and the choices discussed above.

I analysed a specimen of Smithsonian obsidian standard VG-568 several times with each batch ($n > 600$; Table 1). The repeatability for major elements (>10 wt%) was better than 1% relative. For the minor elements (0.1–10 wt%), the repeatability was better than 5% relative, except Fe (which was still better than 10% relative). For the trace elements (<0.1 wt%), the repeatability was over 10% relative and increased as concentrations decreased. This suggests that repeatability becomes poor below the 100 ppm level. Earlier research revealed that trace elements vary by 5–40% relative within an individual flow (Gordus *et al*. 1968; Stross *et al*. 1971), so the observed repeatability was adequate.

Accuracy

Accuracy is the agreement between a measurement and the true (i.e., accepted) value, and it is usually expressed as the per cent relative error. Accuracy is essential if one wishes the data to be compatible with other studies, such as NAA and XRF databases. Consequently, great effort is needed to show the accuracy of any sourcing technique. Accuracy, though, is more difficult to determine than repeatability, because it assumes that one knows the 'true' values. In reality, even the official values for international standards are sometimes disputable. Like repeatability, accuracy in EMPA depends on counting statistics, instrument stability and the above choices.

Table 1 *Repeatability based on Smithsonian Obsidian Standard #VG-568*

	This study		*Per cent relative standard deviation (RSD)*			
	n > 600		*Major*	*Minor*	*Trace*	
	Mean	*SD*	*>10 wt%*	*10–0.1 wt%*	*1000–100 ppm*	*<100 ppm*
SiO_2	76.905	0.353	0.46			
Al_2O_3	12.031	0.103	0.86			
K_2O	5.008	0.075		1.5		
Na_2O	3.679	0.151		4.1		
FeO(T)	1.122	0.110		9.8		
CaO	0.433	0.016		3.7		
Cl	0.098	0.011			11	
TiO_2	0.075	0.009			12	
MgO	0.030	0.005			17	
MnO	0.022	0.008			36	
P_2O_5	0.004	0.008				>100
F	0.002	0.004				>100
SO_3	0.001	0.008				>100
Cr_2O_3	0.000	0.009				>100
Total	99.385	0.373				

To determine accuracy, I used a convergence of approaches, only some of which can be presented here. Comparisons to literature values were limited for three reasons. First, over the decades, researchers have used inconsistent source nomenclature (e.g., the Güneydağ source of Acigöl is also called Güneydağ Tepe, Göl Dağ, Güneş Dağ and even just Acigöl). Second, one cannot assume that two researchers have identical notions of a 'source'. Third, if a source has been little studied, one cannot assume that one or two published data sets are accurate. Instead, I preferred accuracy assessments based on directly comparable specimens.

The first step was to check accuracy against well-characterized standards. To evaluate the major elements, I analysed Smithsonian VG-568 with each batch and compared the data with three published compositions (Table 2). Some values in Jarosewich *et al*. (1980), namely TiO_2 and MnO, are suspect when compared to the other data sets. The per cent relative error, given with respect to the mean published values, was lower than expected from the EMPA literature (Goldstein *et al*. 2003, 392). When the Jarosewich *et al*. (1980) data are excluded, the error is below 20% relative even for elements at low concentrations. To evaluate the trace elements, I analysed two glass standards (NIST SRM #610 and Corning 951RX), compared my data to published data sets (Table 3), and considered the results sufficiently accurate.

I also sought to directly compare my EMPA data to that from XRF and NAA. Obsidian specimens from 12 Mexican sources, sent to me from the MURR Archaeometry Laboratory, served as a 'blind test' because the corresponding NAA and XRF data sets were sent only after my analyses were complete. Table 4 contrasts the XRF, NAA and EMPA data for a sample of these sources. Obsidian from one of these sources, Sierra de Pachuca, was also studied in an inter-laboratory 'round robin' (Glascock 1999). Compared to the mean values from the eight participating laboratories, the EMPA data show favourable agreement (Table 5). The high relative errors for Mg and Ca are due to the extreme variability in the reported values for those elements. Two other comparisons also are ambiguous: F was only measured at one laboratory, and P_2O_5 had markedly different values from just two laboratories.

To compare EMPA, XRF and NAA data from Anatolian and Armenian obsidians from my collection, the MURR Archaeometry Laboratory analysed 94 specimens with NAA and 133 specimens with XRF. Table 6 shows representative data for four Armenian collection areas and good agreement for most elements. Two trends were noticed. First, the Nb and Ga values are higher in the EMPA data than in the XRF data. The values for these elements exhibited good agreement for the standards; however, in the double-digit-ppm range, their accuracies appeared reduced. Hence Nb and Ga were removed from the data analysis. Second, a fraction of the specimens had higher TiO_2, FeO and MnO values in the XRF data, and the same pattern was observed for FeO in the NAA data. Examination of the affected specimens revealed abundant ilmenite [$(Fe,Ti,Mn)O_3$] inclusions measured in XRF and NAA ('whole-rock' techniques), but not in EMPA of the glass matrix alone. This was the only observed case of such an effect. While it does not necessarily preclude compatibility with XRF and NAA databases, the issue of using data from spot techniques with bulk-technique databases (and vice versa) warrants further study to determine if the effects are more significant than other inter-laboratory differences.

Reproducibility

Establishing reproducibility—that is, the degree to which measurements yield identical data when conditions, observers and/or instruments change, or after some period of time has passed—requires procedures to be duplicated by other researchers at different facilities. Any single study

Table 2 *Accuracy based on Smithsonian Obsidian Standard #VG-568*

	This study $n > 600$		*Jarosewich* et al. *(1980)* $n = ?$	*Streck and Wacaster (2006)* $n = 9$		*Rowe* et al. *(2008)* $n = 17$		*Published values with Jarosewich* et al. *(1980)*		*Published values without Jarosewich* et al. *(1980)*	
	Mean	*SD*	*Mean*	*Mean*	*SD*	*Mean*	*SD*	*Mean*	*Relative error (%)*	*Mean*	*Relative error (%)*
SiO_2	76.905	0.353	76.71	76.96	0.53	76.55	0.67	76.74	*0.2%*	76.75	*0.2%*
TiO_2	0.075	0.009	0.12	0.08	0.03	0.08	0.01	0.09	*20%*	0.08	*6.3%*
Al_2O_3	12.031	0.103	12.06	12.17	0.12	12.44	0.19	12.22	*1.6%*	12.30	*2.2%*
Cr_2O_3	0.000	0.009	–	–	–	–	–	–	–	–	–
FeO(T)	1.122	0.110	1.23	1.08	0.05	1.11	0.07	1.14	*1.6%*	1.10	*2.5%*
MnO	0.022	0.008	0.30	0.02	0.02	0.02	0.02	0.11	*81%*	0.02	*10%*
MgO	0.030	0.005	<0.10	0.03	0.02	0.03	0.02	0.03	*0.0%*	0.03	*0.0%*
CaO	0.433	0.016	0.50	0.45	0.03	0.39	0.02	0.45	*3.1%*	0.42	*3.1%*
Na_2O	3.679	0.151	3.75	3.52	0.11	3.51	0.24	3.59	*2.4%*	3.51	*4.7%*
K_2O	5.008	0.075	4.89	4.93	0.2	4.91	0.13	4.91	*2.0%*	4.92	*1.8%*
P_2O_5	0.004	0.008	<0.01	0.00	0.01	0.01	0.01	0.01	*20%*	0.01	*20%*
F	0.002	0.004	–	–	–	–	–	–	–	–	–
SO_3	0.001	0.008	–	0.002	0.002	0.00	0.00	0.00	*0.0%*	0.00	*0.0%*
Cl	0.098	0.011	–	0.101	0.005	0.12	0.01	0.11	*11%*	0.11	*11%*
Total	99.385	0.373	99.44	99.31	0.64	99.18	0.92	99.31	*0.1%*	99.25	*0.1%*

Table 3 *Trace-element analyses of NIST SRM #610 and Corning 951RX glass standards*

	Zr	*Nb*	*Ga*	*Zn*	*Ba*	*Ce*
NIST SRM #610: trace elements in glass						
EMPA—mean	515	522	357	468	561	503
EMPA—SD	30	32	15	29	42	57
Published—mean	444	446	433	455	427	446
Published—SD	12	44	6	30	14	8
EMPA—relative error	16%	17%	18%	3%	31%	13%
Corning 95IRX glass: USNM #117085						
EMPA—mean	5247	23	8	6447	152	–10
EMPA—SD	54	22	12	87	41	46
Published—mean	5820	–	–	6311	152	–
Published—SD	28	–	–	15	–	–
EMPA—relative error	10%	–	–	2%	0%	–

cannot determine the reproducibility of a technique. Consequently, I have laid out my procedures here so that, in conjunction with other recent collaborations, the reproducibility of EMPA-based obsidian sourcing may be determined.

Validity

Neff (1998) has best defined validity in sourcing: 'The instrument is a *valid* indicator to the extent that composition really does measure "source" as a location in geographic space' (116). Repeatability, accuracy and reproducibility may be considered in isolation, but validity involves a context. To determine validity, one must test analytical and data-analysis procedures together using obsidian artefacts from known sources. Therefore, my data-analysis procedures are briefly outlined here.

Scatterplots were used to identify elements most effective for distinguishing sources and exclude either those measured with low repeatability or detrimentally affected by hydration and weathering (Fig. 1). Ultimately, eight elements were chosen for source assignments: Ti, Al, Fe, Mn, Ca, Zr, Zn and Ba. To avoid specifying *a priori* groups, I selected the Euclidean distance (ED), a straightforward multivariate distance measure with no assumptions, as a means of matching artefacts to sources. First, the data were transformed so that major elements did not overwhelm trace ones. Then EDs were calculated between the centroids for each artefact and geological specimen for eight element combinations, varying from three- to seven-dimensional matrices. Assignments followed the procedure: (1) identify the 10 'nearest neighbours' to an artefact for each element combination; (2) identify the most frequent sources among the neighbours; and (3) assign an 'A Rank' to the most frequent nearest source.

I tested the validity of my procedures using eight obsidian artefacts from four Georgian sites. All artefacts were known or expected to originate from Chikiani volcano (Badalyan *et al*. 2004). When my procedures were applied, Chikiani was the 'A Rank' choice over 95% of the time, and all eight artefacts were assigned to Chikiani (i.e., a 100% success rate). Although the test involved only one source, it demonstrated that artefacts may be non-destructively sourced using these procedures (i.e., they are valid). Consequently, the procedures were applied to the 97 Tell Mozan

Table 4 *Examples of comparative EMPA, NAA and XRF data for Mexican specimens*

	Guadalupe Victoria, Puebla						*Malpais, Hidalgo*					
	This study		*NAA—MURR*		*XRF—MURR*		*This study*		*NAA—MURR*		*XRF—MURR*	
	Mean	*SD*	*Mean*	*SD*	*Mean*	*SD*	*Mean*	*SD*	*Mean*	*SD*	*Mean*	*SD*
SiO_2	77.025	0.283					75.940	0.319				
TiO_2	0.099	0.008			0.107	0.015	0.126	0.010			0.131	0.013
Al_2O_3	13.091	0.109					13.409	0.099				
Cr_2O_3	0.000	0.008					0.001	0.008				
FeO	0.466	0.111	0.548	0.008	0.59	0.03	0.862	0.113	0.946	0.014	0.93	0.03
MnO	0.063	0.009	0.067	0.002	0.046	0.005	0.044	0.010	0.054	0.001	0.033	0.007
MgO	0.086	0.008					0.112	0.033				
CaO	0.475	0.030					0.871	0.031				
Na_2O	4.306	0.188	4.41	0.12			4.040	0.171	4.17	0.12		
K_2O	4.093	0.115	4.08	0.20	4.11	0.07	4.125	0.060	4.02	0.23	4.13	0.11
P_2O_5	0.027	0.009					0.033	0.010				
F	0.002	0.003					0.002	0.004				
SO_3	0.000	0.009					0.001	0.009				
Cl	0.077	0.011	0.061	0.011			0.058	0.008	0.051	0.007		
Zr	63	24	54	9	73	5	120	29	96	4	104	8
Nb	65	20			13	3	71	20			14	3
Ga	51	14			12	1	44	18			14	1
Zn	23	54	27	1	28	3	49	40	37	1	35	5
Ba	984	36	931	36			879	34	783	11		
Ce	30	52	27	1			39	56	50	1		

	Otumba, State of Mexico						*Tepalzingo, Hidalgo*					
	This study		*NAA—MURR*		*XRF—MURR*		*This study*		*NAA—MURR*		*XRF—MURR*	
	Mean	*SD*	*Mean*	*SD*	*Mean*	*SD*	*Mean*	*SD*	*Mean*	*SD*	*Mean*	*SD*
SiO_2	75.056	0.423					73.461	0.666				
TiO_2	0.151	0.011			0.177	0.008	0.157	0.018			0.265	0.015
Al_2O_3	13.613	0.119					13.532	0.272				
Cr_2O_3	–0.001	0.008					–0.002	0.008				
FeO	0.977	0.236	1.112	0.019	1.08	0.04	2.276	0.178	2.353	0.026	2.17	0.17
MnO	0.042	0.011	0.049	0.001	0.043	0.011	0.057	0.009	0.063	0.002	0.043	0.008
MgO	0.153	0.072					0.018	0.006				
CaO	1.040	0.058					0.856	0.099				
Na_2O	4.038	0.121	4.00	0.12			4.718	0.308	4.77	0.13		
K_2O	4.221	0.118	4.11	0.25	4.27	0.17	4.474	0.127	4.18	0.24	4.36	0.23
P_2O_5	0.036	0.009					0.007	0.008				
F	0.003	0.004					0.003	0.004				
SO_3	0.000	0.009					–0.001	0.008				
Cl	0.061	0.007	0.056	0.004			0.117	0.010	0.098	0.008		
Zr	137	29	138	7	143	11	472	31	486	14	448	35
Nb	70	23			15	4	97	24			41	5
Ga	48	22			16	1	45	30			23	1
Zn	35	42	40	1	40	5	186	34	146	1	125	8
Ba	865	33	761	15			962	91	892	13		
Ce	35	71	52	1			133	75	138	2		

Table 5 *An inter-laboratory comparison of elemental data for Sierra de Pachuca obsidian*

	This study EMPA			*Overall 'round robin' results Data from Glascock (1999)*				
	Mean	*SD*	*Relative error (%)*	*Mean*	*SD*	*Median*	*Maximum*	*Minimum*
SiO_2	75.7	0.4	0.1	75.6	1.5	75.5	77.4	73.4
TiO_2	0.189	0.010	1	0.187	0.019	0.186	0.217	0.158
Al_2O_3	11.30	0.07	3	11.65	0.77	11.70	12.42	10.43
FeO(T)	2.17	0.03	1	2.16	0.13	2.13	2.43	2.01
MnO	0.140	0.011	2	0.137	0.019	0.141	0.163	0.103
MgO	0.052	0.005	60	0.129	0.128	0.057	0.348	0.047
CaO	0.105	0.019	29	0.147	0.084	0.110	0.330	0.090
Na_2O	5.02	0.30	7	5.38	0.42	5.22	6.11	5.04
K_2O	4.63	0.09	5	4.39	0.39	4.45	5.10	3.75
P_2O_5	0.003	0.009	–	0.025	0.028	0.025	0.045	0.006
F	0.002	0.004	–	0.285	0.019	0.285	0.285	0.285
Cl	0.186	0.010	20	0.155	0.013	0.155	0.165	0.146
Zr	953	40	3	985	84	1005	1097	796
Nb	124	29	31	95	10	91	116	84
Ga	46	16	–	28	4	29	31	23
Zn	291	31	29	225	29	221	292	191
Ba	37	35	–	18	7	17	30	9
Ce	77	42	–	99	17	92	133	90

artefacts. All of the identified sources among the artefacts, including Nemrut Dağ, Bingöl A and B, and Göllü Dağ, were known or suspected to have been used in antiquity, so assignments to those sources are also an indicator of validity. Moreover, no artefacts were attributed to sources rarely, if ever, used in antiquity (e.g., Hasan Dağ and Suphan Dağ), further suggesting validity. The artefacts, the sources and their implications for the site will be discussed in detail elsewhere, but one example follows.

Let us consider artefact A10 q1194.3 f925 k29 (Table 7). For Fe, Ti and Ba, Bingöl B specimens constitute the first seven nearest neighbours. Their ED values are 0.019–0.053. The next two neighbours are specimens from Gutansar, and their ED values increase abruptly: 0.095 and 0.097. The jump indicates that Bingöl B is a superior match compared to Gutansar. This discontinuity in ED values occurs in seven of the element combinations, and Bingöl B is always the 'A Rank' match. Thus, based on its non-destructive analysis, this artefact was assigned to Bingöl B.

CONCLUSIONS

This research expands how EMPA has been used in obsidian sourcing and demonstrates its modern capabilities compared to such well-known studies as Merrick and Brown (1984). In particular, the repeatability and accuracy of the EMPA data show good compatibility with XRF and NAA data from the same specimens and, therefore, the existing databases generated using the two techniques. The results, however, also suggest that, in certain cases, mineral inclusions may lead to differences (although not necessarily detrimental) between measurements with bulk and

Table 6 *Examples of comparative EMPA, NAA and XRF data for four Armenian specimens*

	AR06: Gutansar, Armenia						*AR47: Gutansar, Armenia*					
	This study		*NAA—MURR*		*XRF—MURR*		*This study*		*NAA—MURR*		*XRF—MURR*	
	Mean	*SD*	*Mean*	*SD*	*Mean*	*SD*	*Mean*	*SD*	*Mean*	*SD*	*Mean*	*SD*
SiO_2	74.59	0.11					73.94	0.16				
TiO_2	0.175	0.002			0.300	0.013	0.174	0.002			0.309	0.015
Al_2O_3	13.99	0.04	13.28	0.31			13.91	0.05	13.90	0.47		
Cr_2O_3	0.000	0.002					0.002	0.002				
FeO(T)	1.09	0.01	1.04	0.01	0.967	0.011	1.05	0.02	1.03	0.01	0.996	0.029
MnO	0.077	0.002	0.083	0.001	0.064	0.007	0.075	0.005	0.082	0.001	0.067	0.005
MgO	0.214	0.003					0.199	0.011				
CaO	0.984	0.013					0.976	0.010				
Na_2O	4.37	0.04	4.48	0.09			4.43	0.04	4.39	0.05		
K_2O	4.23	0.03	4.27	0.06	4.16	0.12	4.20	0.03	3.88	0.16	4.19	0.08
P_2O_5	0.034	0.003					0.032	0.001				
F	0.003	0.001					0.005	0.001				
SO_3	0.004	0.003					0.005	0.002				
Cl	0.039	0.002	0.028	0.001			0.040	0.002	0.027	0.001		
Zr	148	6	134	5	174	3	147	6	139	11	182	6
Nb	70	6			29	2	73	18			32	1
Ga	40	4			16	1	33	12			17	1
Zn	82	14	41	1	48	6	58	14	43	1	51	2
Ba	489	9	421	5			486	9	410	19		
Ce	83	14	55	1			97	11	55	1		

	AR41: Pokr Arteni, Armenia						*AR42: Pokr Arteni, Armenia*					
	This study		*NAA—MURR*		*XRF—MURR*		*This study*		*NAA—MURR*		*XRF—MURR*	
	Mean	*SD*	*Mean*	*SD*	*Mean*	*SD*	*Mean*	*SD*	*Mean*	*SD*	*Mean*	*SD*
SiO_2	76.46	0.02					76.32	0.07				
TiO_2	0.076	0.001			0.126	0.003	0.082	0.004			0.088	0.005
Al_2O_3	13.13	0.05	13.60	0.11			12.87	0.01	13.94	0.24		
Cr_2O_3	–0.002	0.001					0.000	0.002				
FeO	0.47	0.00	0.50	0.00	0.616	0.012	0.47	0.01	0.51	0.00	0.621	0.033
MnO	0.076	0.002	0.081	0.001	0.055	0.005	0.071	0.002	0.076	0.002	0.052	0.001
MgO	0.049	0.000					0.054	0.001				
CaO	0.514	0.002					0.515	0.009				
Na_2O	4.22	0.05	4.12	0.02			4.18	0.03	4.10	0.00		
K_2O	4.61	0.03	4.58	0.05	4.52	0.07	4.66	0.01	4.32	0.01	4.48	0.27
P_2O_5	0.010	0.001					0.007	0.001				
F	0.003	0.002					0.001	0.001				
SO_3	0.002	0.001					0.004	0.002				
Cl	0.041	0.000	0.027	0.004			0.039	0.002	0.023	0.000		
Zr	50	8	59	13	87	4	64	2	53	5	89	1
Nb	89	19			30	1	65	1			29	1
Ga	42	11			13	1	40	16			14	1
Zn	99	1	41	1	33	1	88	7	38	1	34	2
Ba	163	11	109	7			283	3	192	12		
Ce	66	13	34	1			55	3	34	1		

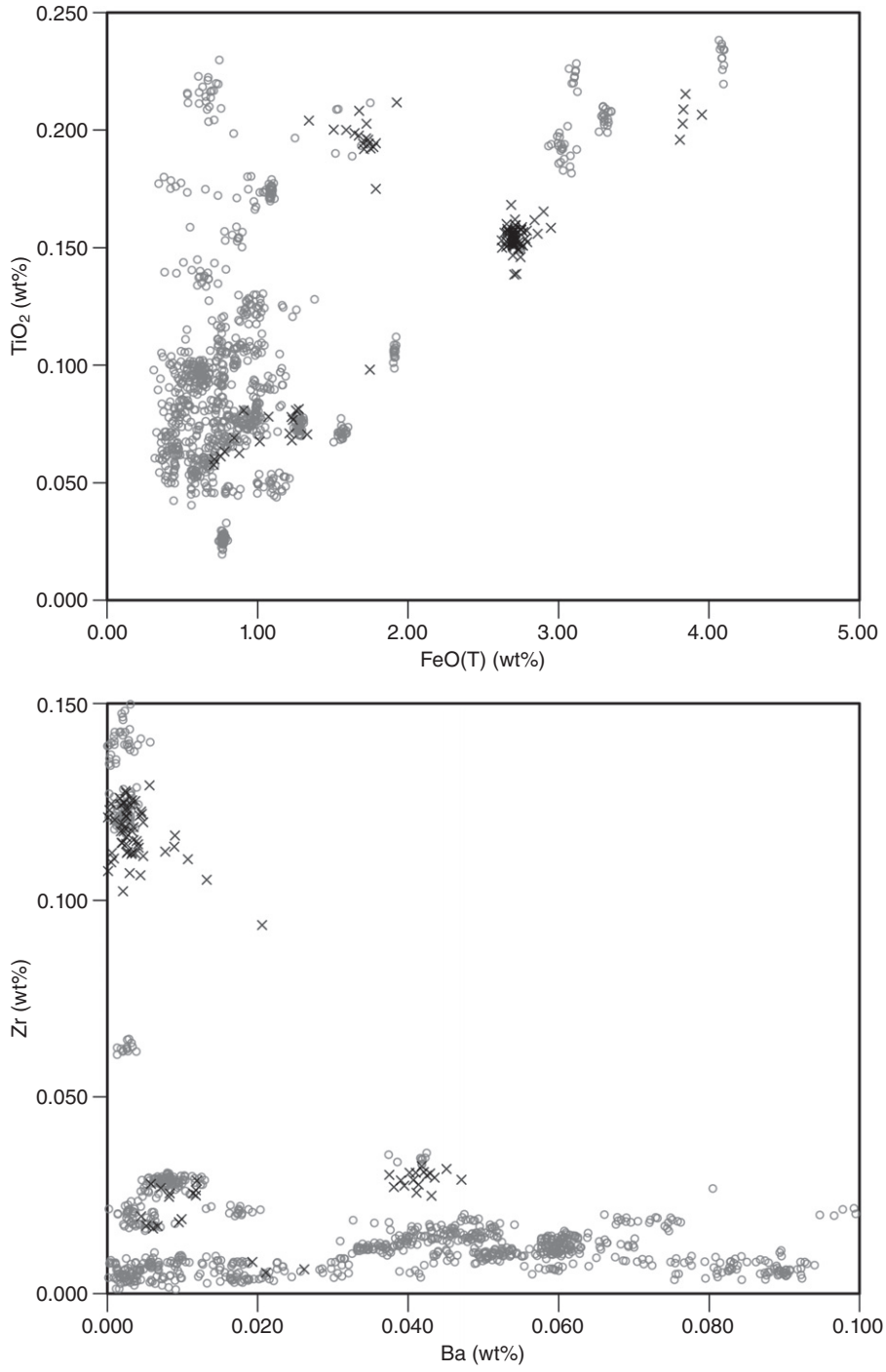

Figure 1 *Example scatterplots reveal some shifts—but small compared to inter-source variations—between the geological specimens (grey circles) and artefacts (black crosses) due to the combined effects of hydration and weathering. Such shifts are even less pronounced in multidimensional space.*

Table 7 *An example of the Euclidean distance calculations for artefact A10 q1194.3 f925 k29 from Tell Mozan, Syria*

A-Rank	**Bingöl B**	**57**	← Of the 80 nearest neighbours to this artefact (10 from each of 8 element combinations), 57 are from Bingöl B
B-Rank	Gutansar	11	

Fe, Ti, Ba			*Fe, Zr, Ba*			*Ti, Fe, Zr, Ba*			*Ti, Fe, Mn, Ca, Zr, Ba*		
A-Rank	**Bingöl B**	**7**	A-Rank	**Bingöl B**	**7**	A-Rank	**Bingöl B**	**7**	A-Rank	**Bingöl B**	**7**
B-Rank	Gutansar	2	B-Rank	Erzincan	3	B-Rank	Gutansar	3	B-Rank	Acigöl	3
Specimen	*Location*	*E.D.*	*Specimen*	*Location*	*E.D.*	*Specimen*	*Location*	*E.D.*	*Specimen*	*Location*	*E.D.*
EA52B1	**Bingöl B**	0.019	EA52B3	**Bingöl B**	0.022	EA52B3	**Bingöl B**	0.029	EA52B2	**Bingöl B**	0.031
EA52B3	**Bingöl B**	0.020	EA52B2	**Bingöl B**	0.025	EA52B2	**Bingöl B**	0.030	EA52B1	**Bingöl B**	0.044
EA52B2	**Bingöl B**	0.021	EA52B1	**Bingöl B**	0.032	EA52B1	**Bingöl B**	0.034	EA53B2	**Bingöl B**	0.048
EA56B1	**Bingöl B**	0.032	EA56B1	**Bingöl B**	0.039	EA53B2	**Bingöl B**	0.044	EA52B3	**Bingöl B**	0.050
EA53B2	**Bingöl B**	0.036	EA53B2	**Bingöl B**	0.041	EA56B1	**Bingöl B**	0.044	EA56B1	**Bingöl B**	0.060
EA53B1	**Bingöl B**	0.045	EA53B1	**Bingöl B**	0.056	EA53B1	**Bingöl B**	0.058	EA53B1	**Bingöl B**	0.068
EA54B1	**Bingöl B**	0.053	EA54B1	**Bingöl B**	0.061	EA54B1	**Bingöl B**	0.062	EA54B1	**Bingöl B**	0.111
AR06E2A	Gutansar	0.095	EA43R2	Erzincan	0.085	AR06E3A	Gutansar	0.140	CA08R1A	Acigöl	0.163
AR06E1A	Gutansar	0.097	EA44P3	Erzincan	0.086	AR30jfL1	Gutansar	0.140	CA08R1C	Acigöl	0.169
AR21avH1	Chazencavan	0.097	EA44P2	Erzincan	0.087	AR06E2A	Gutansar	0.141	CA07R2A	Acigöl	0.174

Fe, Ti, Zr			*Ti, Zr, Ba*			*Ti, Fe, Zr, Ba, Zn*			*Ti, Al, Fe, Mn, Ca, Zr, Ba*		
A-Rank	**Bingöl B**	**7**	A-Rank	**Bingöl B**	**9**	A-Rank	**Bingöl B**	**6**	A-Rank	**Bingöl B**	**7**
B-Rank	Gutansar	2	B-Rank	Erevan	1	B-Rank	Gutansar	4	B-Rank	Acigöl	3
Specimen	*Location*	*E.D.*	*Specimen*	*Location*	*E.D.*	*Specimen*	*Location*	*E.D.*	*Specimen*	*Location*	*E.D.*
EA52B3	**Bingöl B**	0.028	EA52B2	**Bingöl B**	0.027	EA53B1	**Bingöl B**	0.126	EA52B2	**Bingöl B**	0.049
EA52B2	**Bingöl B**	0.029	EA52B3	**Bingöl B**	0.028	EA52B1	**Bingöl B**	0.169	EA53B2	**Bingöl B**	0.051
EA53B2	**Bingöl B**	0.031	EA52B1	**Bingöl B**	0.031	EA52B3	**Bingöl B**	0.182	EA52B1	**Bingöl B**	0.059
EA52B1	**Bingöl B**	0.033	EA54B1	**Bingöl B**	0.032	AR06E2B	Gutansar	0.185	EA52B3	**Bingöl B**	0.064
EA53B1	**Bingöl B**	0.041	EA55B2	**Bingöl B**	0.036	EA54B1	**Bingöl B**	0.194	EA56B1	**Bingöl B**	0.068
EA56B1	**Bingöl B**	0.043	EA56B1	**Bingöl B**	0.038	AR11jB1	Gutansar	0.196	EA53B1	**Bingöl B**	0.070
EA54B1	**Bingöl B**	0.061	EA53B2	**Bingöl B**	0.043	EA52B2	**Bingöl B**	0.198	EA54B1	**Bingöl B**	0.115
EA66W1	Lake Van	0.117	EA55B1	**Bingöl B**	0.047	AR06E1B	Gutansar	0.213	CA08R1A	Acigöl	0.166
AR76rB3	Gutansar	0.126	EA53B1	**Bingöl B**	0.057	AR12jB1	Gutansar	0.213	CA08R1C	Acigöl	0.171
AR06E3A	Gutansar	0.131	AR24jfL1	EDFountain	0.109	EA56B1	**Bingöl B**	0.213	CA07R2A	Acigöl	0.175

spot techniques. Nevertheless, the validity of non-destructive EMPA of obsidian artefacts is shown for the first time in this research. Trace elements were also measured at concentrations below those in earlier EMPA-based obsidian sourcing studies (i.e., below 100 ppm). Therefore, modern EMPA is a valid technique for non-destructively sourcing obsidian artefacts over a range of sizes, including those too small for XRF. Reproducibility will hopefully be accomplished via the publication of these procedures and their successful application in other laboratories.

ACKNOWLEDGEMENTS

Giorgio Buccellati and Marilyn Kelly-Buccellati are the directors of the Tell Mozan excavations under the auspices of the International Institute for Mesopotamian Area Studies. Export of the Tell Mozan artefacts was approved by the Directorate General of Antiquities and Museums, Syrian Arab Republic. The Georgian artefacts were provided by Nino Sadradze and Givi Maisuradze, of the Institute of Geology, and Irina Demetradze, of the Ilia Chavchavadze State University. Many thanks go to Michael Glascock at MURR for providing comparative data. Gilliane Monnier and two anonymous reviewers provided helpful comments that improved the final manuscript.

REFERENCES

Abbès, F., Bellot-Gurlet, L., Cauvin, M. C., Delerue, S., Dubernet, S., Poupeau, G., and Stordeur, D., 2003, Provenance of the Jerf el Ahmar (Middle Euphrates Valley, Syria) obsidians, *Journal of Non-Crystalline Solids*, **323**(1–3), 162–6.

Acquafredda, P., Adriani, T., Lorenzoni, S., and Zanettin, E., 1996, Proposal of a non destructive analytical method by SEM–EDS to discriminate Mediterranean obsidian sources, *Advances in Clay Minerals*, 269–71.

Acquafredda, P., Andriani, T., Lorenzoni, S., and Zanettin, E., 1999, Chemical characterization of obsidians from different Mediterranean sources by non-destructive SEM–EDS analytical method, *Journal of Archaeological Science*, **26**(3), 315–25.

Adams, A. J., Christiansen, E. H., Kowallis, B. J., Carranza-Castaneda, O., and Miller, W. E., 2006, Contrasting silicic magma series in Miocene–Pliocene ash deposits in the San Miguel de Allende Graben, Guanajuato, Mexico, *The Journal of Geology*, **114**, 247–66.

Allan, A. S. R., Baker, J. A., Carter, L., and Wysoczanksi, R. J., 2008, Reconstructing the Quaternary evolution of the world's most active silicic volcanic system: insights from an 1.65 Ma deep ocean tephra record sourced from Taupo Volcanic Zone, New Zealand, *Quaternary Science Reviews*, **27**, 2341–60.

Anovitz, L. M., Elam, J. M., Riciputi, L. R., and Cole, D. R., 1999, The failure of obsidian hydration dating: sources, implications, and new directions, *Journal of Archaeological Science*, **26**, 735–52.

Badalyan, R., Chataigner, C., and Kohl, P., 2004, Trans-Caucasian obsidian: the exploitation of the sources and their distribution, in *A view from the highlands: archaeological studies in honour of Charles Burney* (ed. A. Sagona), 437–65, Peeters, Leuven, Belgium.

Biró, T. K., and Pozsgai, I., 1984, Obszidian lelöhely-azonositas elektronsugaras mikroanalizis segitsegevel (Obsidian characterization by electron microprobe analysis), *Iparregeszet 2 (Industrial Archaeology II)*, 25–38.

Biró, K. T., Pozsgai, I., and Vladár, A., 1986, Electron beam microanalyses of obsidian samples from geological and archaeological sites, *Acta Archaeologica Academiae Scientiarum Hungaricae*, **38**, 257–78.

Bradley, R., 1993, An interview with Colin Renfrew, *Current Anthropology*, **34**(1), 71–82.

Cann, J. R., and Renfrew, C., 1964, The characterization of obsidian and its application to the Mediterranean region, *Proceedings of the Prehistoric Society*, **30**, 111–33.

Carter, T., Poupeau, G., Bressy, C., and Pearce, N., 2006, A new programme of obsidian characterization at Çatalhöyük, Turkey, *Journal of Archaeological Science*, **33**(7), 893–909.

Coote, G. E., and Nistor, P., 1982, Depth profiles of sodium in obsidian by the resonant nuclear reaction method: a potential dating method, in *Archaeometry: an Australian perspective* (eds. W. Ambrose and P. Duerden), The Australian National University Press.

Eerkens, J. W., King, J., and Glascock, M. D., 2002, Artifact size and chemical sourcing: studying the potential biases of selecting large artifacts for analysis, *Society for California Archaeology Newsletter*, **36**(3), 25–9.

Frahm, E., 2010, *The Bronze-Age obsidian industry at Tell Mozan (ancient Urkesh), Syria: redeveloping electron microprobe analysis for 21st-century sourcing research and the implications for obsidian use and exchange in northern Mesopotamia after the Neolithic*, Ph.D. dissertation, Department of Anthropology, University of Minnesota–Twin Cities.

Frahm, E., in press, Evaluation of archaeological sourcing techniques: reconsidering and re-deriving Hughes' four-fold assessment scheme, *Geoarchaeology*.

Freestone, I. C., 1982, Applications and potential of electron probe microanalysis in technological and provenance investigations of ancient ceramics, *Archaeometry*, **24**, 99–116.

Friedman, I., Smith, R. L., and Clark, D., 1969, Obsidian dating, in *Science in archaeology* (eds. D. R. Brothwell and E. Higgs), 62–75, Praeger, New York.

Glascock, M. D., 1999, An inter-laboratory comparison of element compositions for two obsidian sources, *International Association for Obsidian Studies Bulletin*, **23**, 13–25.

Goldstein, J. I., Newbury, D. E., Echlin, P., Joy, D. C., Fiori, C., and Lifshin, E., 1981, *Scanning electron microscopy and X-ray microanalysis: a text for biologists, materials scientists, and geologists*, 1st edn, Plenum Press, New York.

Goldstein, J. I., Newbury, D. E., Joy, D. C., Lyman, C. E., Echlin, P., Lifshin, E., Sawyer, L., and Michael, J. R., 2003, *Scanning electron microscopy and X-ray microanalysis*, 3rd edn, Springer, New York.

Gordus, A. A., Wright, G. A., and Griffin, J. B., 1968, Obsidian sources characterized by neutron-activation analysis, *Science*, **161**(3839), 382–4.

Gordus, A. A., Fink, W. C., Hill, M. E., Purdy, J. C., and Wilcox, T. R., 1967, Identification of the geologic origins of archaeological artifacts: an automated method of Na and Mn neutron activation analysis, *Archaeometry*, **10**, 87–96.

Hang, T., Wastegard, S., Veski, S., and Heinsalu, A., 2006, First discovery of cryptotephra in Holocene peat deposits of Estonia, eastern Baltic, *Boreas*, **35**, 644–9.

Hanson, B., Delano, J. W., and Lindstrom, D. J., 1996, High-precision analysis of hydrous rhyolitic glass inclusions in quartz phenocrysts using the electron microprobe and INAA, *American Mineralogist*, **81**, 1249–62.

Hughes, R. E., 1998, On reliability, validity, and scale in obsidian sourcing research, in *Unit issues in archaeology: measuring time, space, and material* (eds. A. F. Ramenofsky and A. Steffen), 103–14, University of Utah Press, Salt Lake City, UT.

Hunt, J., and Hill, P., 2001, Tephrachronological implications of beam size: sample-size effects in electron microprobe analysis of glass shards, *Journal of Quaternary Science*, **16**(2), 105–17.

Hurcombe, L. M., 1992, *Use wear analysis and obsidian: theory, experiments, and results*, J. R. Collis Publications, Sheffield.

Jarosewich, E., Nelen, J. A., and Norberg, J. A., 1980, Reference samples for electron microprobe analysis, *Geostandards Newsletter*, **4**, 43–7.

Keller, J., and Seifried, C., 1990, The present status of obsidian source identification in Anatolia and the Near East, in *Volcanology and archaeology, proceedings of the European Workshops of Ravello, PACT*, **25**, 57–87.

Kempe, D. R. C., and Templeman, J. A., 1983, Techniques, in *The petrology of archaeological artifacts* (eds. D. R. C. Kempe and A. P. Harvey), 26–52, Clarendon Press, Oxford.

Kerrick, D. M., Eminhizer, L. B., and Villaume, J. F., 1973, The role of carbon film thickness in electron microprobe analysis, *American Mineralogist*, **58**, 920–5.

Le Bourdonnec, F.-X., Poupeau, G., and Luglie, C., 2006, SEM–EDS analysis of Western Mediterranean obsidians: a new tool for Neolithic provenance studies, *Comptes Rendus—Géoscience*, **338**(16), 1150–7.

Le Bourdonnec, F.-X., Poupeau, G., and Luglie, C., 2010, The Monte Arci (Sardinia, Western Mediterranean) obsidians: characterization by multivariate analysis from SEM–EDS, EMP–WDS and PIXE elemental compositions, in *L'ossidiana del Monte Arci nel Mediterraneo. Nuovi Apporti Sulla Diffusione, sui Sistemi di Produzione e Sulla Loro Cronologia, Atti del 5° Convegno Internazionale (Pau, Italia, 27–29 Giugno 2008)*, 13–28.

Le Bourdonnec, F.-X., Lugliè, C., Dubernet, S., Bohn, M., and Poupeau, G., 2005, Monte Arci (Sardinia) obsidians: new geochemical data from electron microprobe and ion beam analysis, *Le vie dell'ossidiana nel Mediterraneo ed in Europa, Atti del 3° Convegno Internazionale, Pau, Italy, 25–26 September 2004, PTM, Mogoro.*

Lifshin, E., and Gauvin, R., 2001, Minimizing errors in electron microprobe analysis, *Microscopy & Microanalysis*, **7**(2), 168–77.

Long, J. V. P., 1995, Microanalysis from 1950 to the 1990s, in *Microprobe techniques in the Earth sciences* (eds. P. J. Potts, J. F. Bowles, S. J. B. Reed and R. Cave), 1–48, Chapman & Hall, London.

Merrick, H., and Brown, F., 1984, Rapid chemical characterization of obsidian artifacts by electron microprobe analysis, *Archaeometry*, **26**, 230–6.

Neff, H., 1998, Units in chemistry-based ceramic provenance investigation, in *Unit issues in archaeology: measuring time, space, and material* (eds. A. F. Ramenofsky and A. Steffen), 115–27, University of Utah Press, Salt Lake City, UT.

Patel, S., Hedges, R., and Kilner, J., 1998, Surface analysis of archaeological obsidian by SIMS, *Journal of Archaeological Science*, **25**(10), 1047–54.

Payne, R., Blackford, J., and van der Plicht, J., 2008, Using cryptotephras to extend regional tephrochronologies: an example from southeast Alaska and implications for hazard assessment, *Quaternary Research*, **69**, 42–55.

Poupeau, G., Le Bourdonnec, F.-X., Carter, T., Delerue, S., Shackley, M. S., Barrat, J.-A., Dubernet, S., Moretto, P., Calligaro, T., Mili, M., and Kobayashi, K., 2010, The use of SEM–EDS, PIXE, and EDXRF for obsidian provenance studies in the Near East: a case study from Neolithic Çatalhöyük (Central Anatolia), *Journal of Archaeological Science*, **37**, 2705–20.

Reed, S. J. B., 1993, *Electron microprobe analysis*, 2nd edn, Cambridge University Press, Cambridge, UK.

Reed, S. J. B., 2005, *Electron microprobe analysis and scanning electron microscopy in geology*, 2nd edn, Cambridge University Press, Cambridge, UK.

Rosen, S. A., Tykot, R., and Gottesman, M., 2005, Long distance trinket trade: Early Bronze Age obsidian from the Negev, *Journal of Archaeological Science*, **32**(5), 775–84.

Rowe, M. C., Thornber, C. R., Gooding, D. J., and Pallister, J. S., 2008, *Catalog of Mount St. Helens 2004–2005 tephra samples with major- and trace-element geochemistry*, Volcano Hazards Program, US Geological Survey.

Sanna, I., Le Bourdonnec, F.-X., Poupeau, G., and Luglie, C., 2010, Ossidiane non sarde in Sardegna: analisi di un rinvenimento subacqueo nel Porto di Cagliari, in *L'ossidiana del Monte Arci nel Mediterraneo. Nuovi apporti sulla diffusione, sui sistemi di produzione e sulla loro cronologia, atti del 5° Convegno Internazionale (Pau, Italia, 27–29 Giugno 2008)*, Ales, Italy.

Smith, H. W., Okazaki, R., and Knowles, C. R., 1977, Electron microprobe data for tephra attributed to Glacier Peak, Washington, *Quaternary Research*, **7**, 197–206.

Stevenson, D. P., Stross, F. H., and Heizer, R. F., 1971, An evaluation of X-ray fluorescence analysis as a method for correlating obsidian artifacts with source location, *Archaeometry*, **13**, 11–16.

Streck, M., and Wacaster, S., 2006, Plagioclase and pyroxene hosted melt inclusions in basaltic andesites of the current eruption of Arenal Volcano, Costa Rica, *Journal of Volcanology and Geothermal Research*, **157**(1–3), 236–53.

Stross, F. H., Stevenson, D. P., Weaver, J. R., and Wyld, G., 1971, Analysis of American obsidians by X-ray fluorescence and neutron activation analysis, in *Science and Archaeology* (ed. R. H. Brill), 210–21, The MIT Press, Cambridge, MA.

Summerhayes, G., Bird, J. R., Fullagar, R., Gosden, C., Specht, J., and Torrence, R., 1998, Application of PIXE–PIGME to archaeological analysis of changing patterns of obsidian use in west New Britain, Papua New Guinea, in *Archaeological obsidian studies: method and theory* (ed. M. S. Shackley), 129–58, Plenum Press, New York.

Tryon, C., Logan, M., Mouralis, D., and Kuhn, S., 2009, Building a tephrostratigraphic framework for the Paleolithic of central Anatolia, Turkey, *Journal of Archaeological Science*, **36**, 637–52.

Tykot, R. H., 1995, *Prehistoric trade in the Western Mediterranean: the sources and distribution of Sardinian obsidian*, Ph.D. dissertation, Harvard University.

Tykot, R. H., and Chia, S., 1997, Long-distance obsidian trade in Indonesia, in *Materials issues in art and archaeology V* (eds. P. B. Vandiver, J. R. Druzik, J. F. Merkel and J. Stewart), 175–80, Materials Research Society Symposium Proceedings, vol. 462, Materials Research Society, Pittsburgh, PA.

Wada, K., 2009, Petrologic model of Shirataki obsidian, northern Hokkaido, Japan: its structure, composition and the origin, in *Geological Society of America Abstracts with Programs*, **41**, 553, Portland, OR.

Weisler, M. I., and Clague, D. A., 1998, Characterisation of archaeological volcanic glass from Oceania: the utility of three techniques, in *Archaeological obsidian studies: method and theory* (ed. M. S. Shackley), 103–28, Springer, New York.

Yanagisawa, N., Fujimoto, K., Nakashima, S., Kurata, Y., and Sanada, N., 1997, Micro FT–IR study of the hydration-layer during dissolution of silica glass, *Geochimica et Cosmochimica Acta*, **61**, 1165–70.